Nonlinear model predictive control for optimal dose administration in radiotherapy

João C. G. Araújo[1], Bruno J. Guerreiro[1,2], Luis B. Oliveira[1], and Filipe Ferreira da Silva[3]

[1] LASI, CTS-UNINOVA and Department of Electrical and Computer Engineering, NOVA School of Science and Technology, 2829-516 Caparica, Portugal
[2] Institute For Systems and Robotics, LARSyS, 1049-001 Lisbon, Portugal
[3] CEFITEC, Department of Physics, NOVA School of Science and Technology, 2829-516 Caparica, Portugal

Abstract. Radiotherapy is one of the main treatments for oncological disease. Several mathematical models have been put forward in an attempt to describe the effect of radiation dose on tumor growth dynamics. This work discusses the nonlinear modeling of healthy and cancer cell population growth under the influence of radiotherapy, and proposes predictive control techniques to determine the optimal dose for tumor control, while sparing surrounding healthy tissue. Radiation effects are modelled by a linear-quadratic formalism, coupled with a novel population-specific delayed dose response. Numerical simulations of the open- and closed-loop system are conducted, and robustness against model uncertainty is studied. Results illustrate the controller's performance when dealing with imperfect information and unexpected system behavior, and how it can be tuned to produce the desired treatment outcome. However, optimal operation is conditioned by a limited prediction horizon, as well as strict adherence to treatment schedules and dose restrictions.

Keywords: Radiotherapy · model predictive control · nonlinear systems.

1 Introduction

Cancer is one of the leading causes of death worldwide, and the subject of active research across different fields. Several treatments have been developed over the last decades in an effort to control tumor growth, though toxicity management and long-term efficacy are still ongoing concerns. Out of these procedures, radiotherapy (RT) is one of the oldest and most widely employed [8]. In RT, a beam of ionizing radiation is targeted at the cancer tissue; the amount of energy deposited per mass of tissue is called the absorbed dose, and is measured in units of joule per kilogram, or gray (Gy). Exposure to ionizing radiation affects living tissue by inducing DNA lesions in the cell. If left unrepaired, this damage will compromise the afflicted cell's ability to self-replicate through mitosis, "killing" it by way of mitotic catastrophe or apoptosis [1]. Since cancer cells generally proliferate much faster than regular cells, their rate of death due to radiation-induced damage is also higher, and so they are said to be more radiosensitive [8].

Mathematical modelling of cancer growth and treatment has systematically contributed to greater clinical success rates and improved patient outcomes [13], but relatively little has been said concerning the application of automatic control algorithms. While some optimal control solutions have been recently studied, the existing body of work is mostly concerned with mathematical analysis rather than practical application, and consequently remains largely academical [7,3]. A further unexplored branch of this subject is the implementation of closed-loop predictive techniques for real-time control.

The main contribution of this work is the proposed model predictive control strategy for optimizing dose delivery in RT, based on a modified competition model of tissue dynamics. Open- and closed-loop numerical simulations are conducted, and the effects of controller tuning on final outcomes are briefly discussed. Robustness against uncertainty and disturbances, such as different patient reactions to an equivalent therapy, is also demonstrated.

The remainder of the article is structured as follows: Section 2 presents the system model, which is subsequently developed by introducing a radiation response term and a distributed delay; Section 3 deals with controller design and implementation, and discusses simulation results; finally, Section 4 concludes the work by summarizing the strengths and limitations of the proposed system, and offering prospects for future research.

2 The Model

The competition among a certain number of species for a common resource can be modelled by a system of logistic growth equations modified by death rate terms due to inter-species competition [12]. These concepts were applied in [4] to describe the interaction between normal and tumor cells, with the two populations competing for common tissue nutrients.

2.1 Competition

The populations of normal cells and cancer cells in a given volume of tissue, x_n and x_c respectively, are described by the two species competitive system [4,9]

$$\dot{x}_n = a_n x_n \left(1 - \frac{x_n}{K_n}\right) - b_n x_n x_c \tag{1a}$$

$$\dot{x}_c = a_c x_c \left(1 - \frac{x_c}{K_c}\right) - b_c x_n x_c \tag{1b}$$

where $\dot{x}$ denotes the derivative of x with respect to time. Eq. (1) will be dubbed the Belostotski-Freedman model (BFM). The variables x_n and x_c can equivalently express cell number or tissue volume, and the latter interpretation will be considered throughout. The meaning and value of each parameter in (1) is summarized in Table 1. Given the BFM's biological interpretation, it follows that

$$0 \leq x_{n,c} \leq K_{n,c}, \quad a_{n,c}, b_{n,c} \geq 0, \quad K_{n,c} > 0 \ . \tag{2}$$

Table 1: Parameter values for the BFM.

Param.	Value	Definition
a_n	3.13×10^{-4} hour^{-1}	Intrinsic growth rate of normal cells.
a_c	6.25×10^{-4} hour^{-1}	Intrinsic growth rate of cancer cells.
b_n	1.56×10^{-5} cm^{-3} hour^{-1}	Effect of competition on normal cells.
b_c	6.25×10^{-6} cm^{-3} hour^{-1}	Effect of competition on cancer cells.
K_n	20 cm^3	Normal cell carrying capacity.
K_c	20 cm^3	Cancer cell carrying capacity.

Some discussion of the values listed in Table 1 is warranted. Parameters in cancer modelling are often estimated by fitting clinical data, meaning values can vary greatly according to cancer type and patient characteristics, often spanning multiple orders of magnitude [16]. The present model values were chosen based on prior literature, and tweaked for the sake of presenting interesting examples: a_c is based on [16], where a logistic model of tumor growth was fitted to clinical data for head and neck cancer patients; a_n was taken to be $a_c/2$, since regular tissue is generally expected to exhibit less activity than tumor tissue; the value for K_c was based on [16] and the relation $K_n = K_c$ was assumed; finally, $b_n = a_n/K_c$ and $b_c = a_c/5K_n$ [4], the latter of which was tailored alongside a_c to simulate an early tumor doubling time of around 50 days.

The dynamics of (1) were simulated in Matlab using the built-in function `ode45`. A time series and phase-space plots for various initial conditions are illustrated in Fig. 1a and 1b, respectively. Extensive study of the model's properties, including stability and equilibria, has been carried out in prior literature [4,9], and is not replicated in the present work. Rather, the set of simulations in Fig. 1 is meant to illustrate that, for the parameter values of Table 1, the system (1) evolves toward a cancer-dominated state.

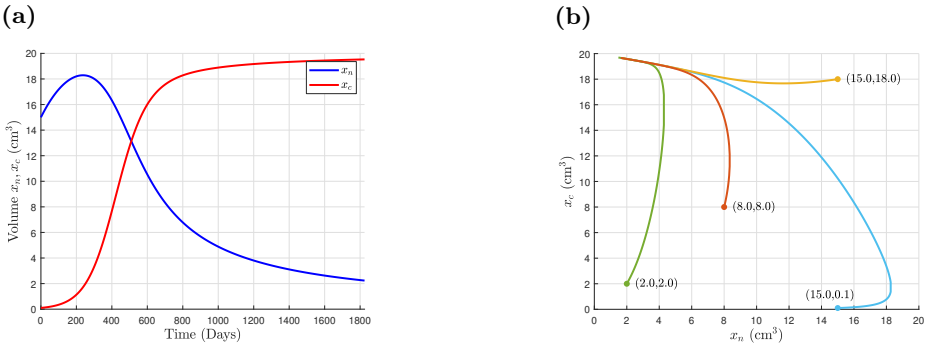

Fig. 1: Numerical simulation of the behavior of system (1). (a) Time series, with initial conditions $x_0 = (15, 0.1)$. (b) Phase portrait for various initial conditions.

2.2 Radiation response

The BFM can be modified to account for treatment conditions by adding a death rate term to the original equations

$$\dot{x}_n = a_n x_n \left(1 - \frac{x_n}{K_n}\right) - b_n x_n x_c - c_n x_n \tag{3a}$$

$$\dot{x}_c = a_c x_c \left(1 - \frac{x_c}{K_c}\right) - b_c x_n x_c - c_c x_c \ . \tag{3b}$$

Analogous to the growth rates $a_{n,c}$, the death rates $c_{n,c}$ negatively impact the cells' proliferation by accounting for the damage induced by radiation. In order to correlate $c_{n,c}$ to the administered radiation dose, the approach proposed by [16] will be used. Assuming the standard linear-quadratic relation between absorbed dose $D_{n,c}$ and survival probability [13],

$$c_{n,c} = 1 - e^{-\left(\alpha_{n,c} D_{n,c} + \beta_{n,c} D_{n,c}^2\right)} \tag{4}$$

where $\alpha_{n,c}$ and $\beta_{n,c}$ are weights relating to the exposed cells' radiosensitivity (see Table 2). The absorbed dose is given by the continuous summation of the time-varying dose rate $d_{n,c}(t)$ over the administration period, and can be described by the differential equation

$$\dot{D}_{n,c} = d_{n,c} - D_{n,c} \ . \tag{5}$$

Parameter values for (4) are summarized in Table 2. The value for α_c is based on the fitting of clinical data in [16] for head and neck cancer. The cancer cells were assumed to have a α_c/β_c ratio of 10 Gy, which is typical for rapidly proliferating tissue [13]. On the other hand, the normal tissue was considered to be more resistant to the effects of radiation, hence $\alpha_n = \alpha_c/2$; moreover, the normal tissue was modelled by a α_n/β_n ratio of 1 Gy, concomitant with its greater repair capability [13,1]. With contemporary technology, the radiation dose absorbed by regular cells is expected to be much smaller than that of cancer cells, i.e. $D_n \ll D_c$, and would ideally be 0. However, the (rather pessimistic) assumption will be made throughout that $D_n = D_c/3$, or equivalently $d_n = d_c/3$ [11]. Given this presupposition, the indices in d_c and D_c will be suppressed in subsequent notation.

2.3 Distributed delay

To further expand upon the death rate model of (4), let us now consider the fact that, generally, the effects of radiation upon biological tissue are not immediately made manifest. In RT, significant cell death may only occur a few hours, or days, after the treatment session [16,10]. Thus, it is sensible to incorporate such a delay into (4). Since gamma distributions arise in a variety of biological systems, and have recently been correlated to the statistics of radiation-induced DNA

Table 2: Treatment parameter values.

Param.	Value	Definition
α_n	1.12×10^{-2} Gy^{-1}	Effect of lethal events in normal cell survival.
α_c	2.23×10^{-2} Gy^{-1}	Effect of lethal events in cancer cell survival.
β_n	1.12×10^{-2} Gy^{-2}	Effect of sub-lethal damage in normal cell survival.
β_c	2.23×10^{-3} Gy^{-2}	Effect of sub-lethal damage in cancer cell survival.
μ	2 hours	Average delay between first exposure and cell death.
d	8 Gy hour^{-1}	Absorbed dose rate.
D	2 Gy	Total dose per treatment session.
D_T	70 Gy	Total administered dose.

damage [5], a distributed gamma-type delay given by [15]

$$\begin{aligned} d * g_\lambda^\nu &= \int_{-\infty}^{t} d(\tau) g_\lambda^\nu (t-\tau)\, d\tau \\ &= \int_{-\infty}^{t} d(\tau) \frac{\lambda^\nu (t-\tau)^{\nu-1} e^{-\lambda(t-\tau)}}{\Gamma(\nu)}\, d\tau \end{aligned} \tag{6}$$

was considered. Here, Γ is the gamma function, and ν and λ are the shape and rate parameters of the gamma distribution, respectively. The average delay is given by the mean value of the density function, $\mu = \nu/\lambda$, with variance $\sigma^2 = \nu/\lambda^2$ [15]. To improve computational tractability, the convolution integral (6) can be represented by a system of differential equations by using the so-called "linear chain trick." Let $D_\nu = d * g_\lambda^\nu$. Then, it can be shown that [15]

$$\dot{D}_0 = \lambda\,(d - D_0) \tag{7a}$$

$$\dot{D}_i = \lambda\,(D_{i-1} - D_i)\,, \quad 1 \le i \le \nu\ . \tag{7b}$$

This elegant formulation expands the convolution integral into $\nu + 1$ differential equations, which can be solved alongside the two BFM state equations.

2.4 Final model

By assimilating (4) and (7) into (3), the expanded BFM is described by

$$\dot{x}_n = a_n x_n \left(1 - \frac{x_n}{K_n}\right) - b_n x_n x_c - x_n \left[1 - e^{-\left(\alpha_n D_\nu + \beta_n D_\nu^2\right)}\right] \tag{8a}$$

$$\dot{x}_c = a_c x_c \left(1 - \frac{x_c}{K_c}\right) - b_c x_n x_c - x_c \left[1 - e^{-\left(\alpha_c D_\nu + \beta_c D_\nu^2\right)}\right] \tag{8b}$$

$$\dot{D}_0 = \lambda\,(d - D_0) \tag{8c}$$

$$\dot{D}_i = \lambda\,(D_{i-1} - D_i)\,, \quad 1 \le i \le \nu\ . \tag{8d}$$

Note how (8c) resembles (5): by setting $\nu = 0$ and $\lambda = 1$, the formulation from (5) is recovered and the delay is nullified. Otherwise, for mean delay $\mu > 0$, ν was estimated as 2^{μ}; λ is simply given by ν/μ. Although the formulation in (8) assumes the same delay for both state variables, by using the nth to last equation $D_{\nu-n}$ instead of D_{ν} in (8a) and/or (8b), multiple combinations of delay length/shape can be selected.

In an effort to replicate the conditions of real treatment, the system (8) was numerically simulated with the parameters in Table 2, based on data pertaining to head and neck cancer patients. The treatment plan consists of 15 min weekday sessions of 2 Gy each, amounting to a total dose D_T of 70 Gy over the course of 7 weeks [16,11]. The system's response to the same total dose delivered continuously over 8 hours and 45 min (equivalent to all 15 min sessions back to back) was also simulated. Fig. 2a and 2b depict the two scenarios, respectively, for two different delay values. It is apparent that the same dose administered over a shorter period of time results in greater damage to the surrounding healthy tissue. This behavior is a consequence of the linear-quadratic model used in (4), and accurately predicts the benefits of "fractionation" (i.e. splitting a large dose into many shorter exposures), which has long been standard clinical practice [13,8].

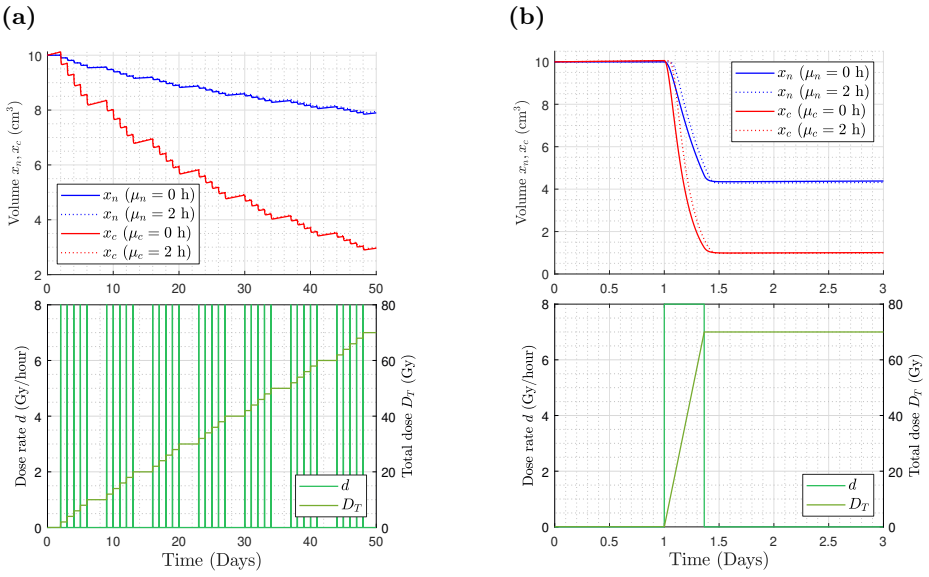

Fig. 2: Simulation of the model (8) for two different treatment modalities, both with initial conditions $x_0 = (10, 10)$. (a) Conventionally fractioned treatment. (b) Highly concentrated dose delivery.

3 The Controller

In the previous section, practical RT treatment was modelled as a prescribed absorbed dose fractioned into a series of short, constant dose exposures over a long period of time. By taking the dose rate as an input variable, control strategies can be devised to adjust radiation intensity according to various criteria. In this section, the design of a dose rate controller for optimal cell regulation is demonstrated.

3.1 Model predictive control

Model predictive control (MPC) is a closed-loop technique that utilizes predictions of the controlled system's behavior to drive it along the trajectory that will minimize a specified cost functional [6]. At any given sampling instant, the controller uses its model of the system, along with all information available up to a point in the future, to solve an optimal control problem, while adjusting its predictions to the real system's response. Since the system (8) is highly nonlinear, a nonlinear MPC (NMPC) strategy was adopted.

3.2 Design and implementation

NMPC is typically implemented as a discrete-time control strategy, and hence requires a discrete-time system model. Let us write (8) in state-space form as

$$\dot{x} = \left[\dot{x}_n \; \dot{x}_c \; \dot{D}_0 \ldots \dot{D}_\nu\right]^T = f\left(x, d\right), \quad y = \left[x_n \; x_c\right]^T \tag{9}$$

where x is the state vector, f is the nonlinear system function and y is the output vector. The system (9) can be discretized by an explicit Euler method

$$x_{k+1} = x_k + T_s f\left(x_k, d_k\right), \quad y_k = \left[x_{k_n} \; x_{k_c}\right]^T \tag{10}$$

where k is an instant in time and T_s is the controller's sampling period. The controller uses (10) to predict the system's behavior up to a number of sample times ahead; at each subsequent instant, this prediction horizon recedes further into the future by another T_s. For a prediction horizon of N samples, the cost functional J was chosen to be of the quadratic form

$$J(x_k, d_k) = \sum_{k=0}^{N-1} -w_n x_{k_n}^2 + w_c x_{k_c}^2 + w_d d_k^2 + w_r (d_k - d_{k-1})^2 \tag{11}$$

where w_n, w_c, w_d and w_r are the weights on normal cell volume, cancer cell volume, dose rate and dose rate variation, respectively; since the optimization algorithm seeks to minimize the value of J, the minus sign in front of w_n ensures that the number of normal cells is maximized. All weights are ≥ 0, and are assumed to remain constant in time. The optimization problem consists of minimizing J while subject to a number of constraints, chief among these being the dynamic

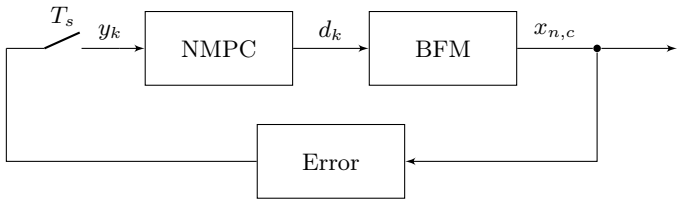

Fig. 3: Functional block diagram of the closed-loop system.

constraint imposed by the model (10). The physical interpretation of the system's variables also impose certain natural limitations, as in (2). In addition, further constraints were added to keep the optimization space in reasonable accordance with practical scenarios. Namely, an upper bound $d_{k_{max}}$ was introduced to keep the dose rate fairly low, while still allowing some room for adjustment; a limit on the total dose D_T was also imposed in certain scenarios. The optimization problem to be solved at each sample interval can thus be stated as

$$\begin{aligned} \min_{d_0,\cdots,d_{N-1}} \quad & J(x_k, d_k) \\ \text{subject to} \quad & x_{k+1} = x_k + T_s f\left(x_k, d_k\right) \\ & y_k = x_k \\ & x_0 = x(0) \\ & 0 \leq x_{k_{n,c}} \leq K_{n,c} \\ & 0 \leq d_k \leq d_{k_{max}} \\ & D_T = \int d_k \leq D_{T_{max}} \ . \end{aligned} \tag{12}$$

The controller was implemented in Matlab using the built-in optimization framework, and coupled to the system (8) as depicted in Fig. 3. The controller samples the system's output at regular intervals of T_s, each time computing the optimal dose rate d_k that will satisfy (12). To model the uncertainty inherent in measuring/estimating tissue volumes, an error was introduced in the feedback loop. This uncertainty takes the form of the element-wise product

$$y_k = x_{n,c}(1 + e) \tag{13}$$

where the error $e \in \mathbb{R}^{2\times 1}$ is randomly sampled from a normal distribution with 0 mean and standard deviation $\sigma = 0.1$, implying that $\sim 2/3$ of measurements are within $\pm 10\%$ error. As before, the BFM was parameterized with the values from Tables 1 and 2, except that the cancer cells were now assumed to begin responding to radiation sooner than the healthy ones, such that $\mu_c = 1$ hour and $\mu_n = 2$ hours. The controller was configured with a fixed sampling time of $T_s = 15$ min and a prediction horizon N of 9 samples (estimated as $\lceil (15 \text{ min} + \mu_n)/T_s \rceil$) , but the weights and constraints in (11) and (12) were adjusted according to different simulation scenarios.

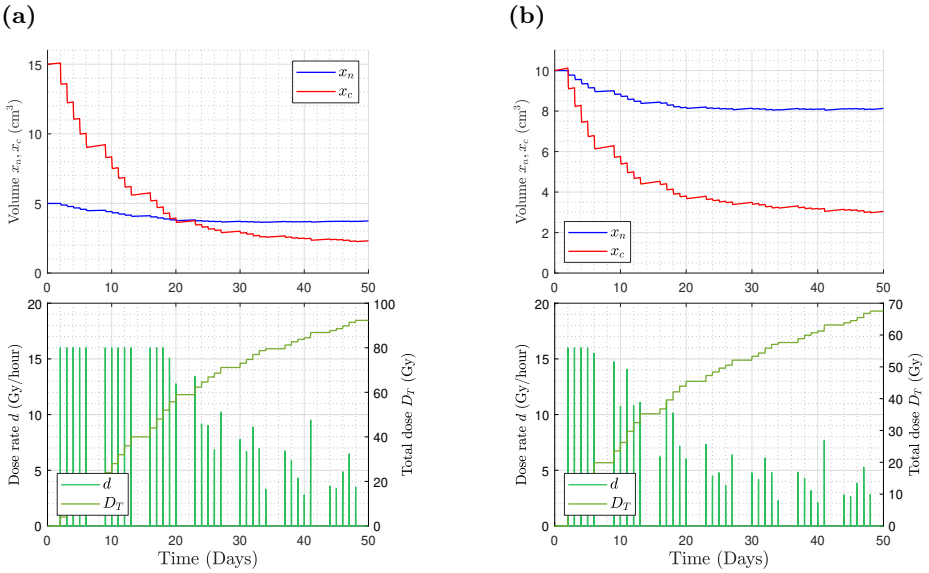

Fig. 4: Simulation of the closed-loop system for different weights and initial conditions, in a pulsed control regimen. (a) $x_0 = (5, 15)$, weights $= (1, 2, 0.1, 0)$. (b) $x_0 = (10, 10)$, weights $= (1, 5, 0.5, 0)$.

3.3 Simulation and Discussion

The closed-loop system was first simulated in the conventional RT regimen described previously, i.e., 15 min weekday sessions for 7 weeks in a row. Numerically, these sessions were implemented by periodically changing $d_{k_{max}}$ from 16 Gy/hour (treatment conditions, but around twice the regular rate) to 0 (no treatment); this change was incorporated into the controller's prediction horizon, for optimal operation. Fig. 4 illustrates the results from two simulations conducted for different stages of cancer development, with different control weights. In each set of results, the respective weights are presented in the form (w_n, w_c, w_d, w_r). Fig. 4a shows a closed-loop solution with similar results as those of the conventional treatment simulated in Fig. 2. In Fig. 4b, greater priority was assigned to eliminating tumor cells, though this was tempered by a somewhat higher weight on radiation usage, as well.

The treatment regime offers a very rigid control structure, and somewhat limits the assessment of the controller's performance. Hence, in the next set of simulations the treatment schedule was discarded altogether and the controller was allowed to operate "continuously." The results for two sets of initial conditions and weights are depicted in Fig. 5. Here, $d_{k_{max}}$ was set to a low 150 cGy/hour and a $D_{T_{max}}$ of 80 Gy was imposed. Additionally, a large weight was placed on dose rate variation, since the random measurement errors would otherwise produce a very erratic control. Fig. 5a shows an aggressive initial response, which

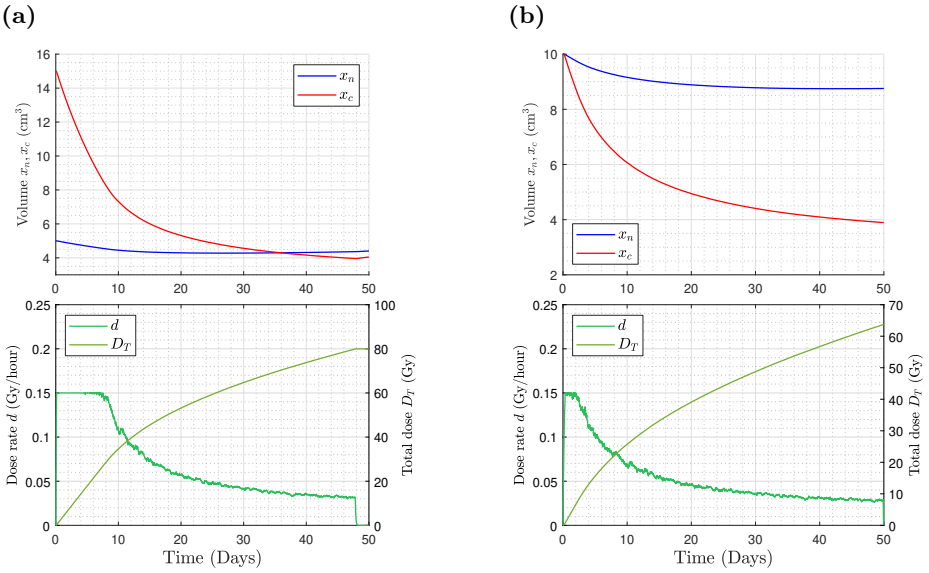

Fig. 5: Simulation of the closed-loop system for different weights and initial conditions, in an uninterrupted control mode. (a) $x_0 = (5, 15)$, weights $= (1, 4, 19, 5 \times 10^3)$. (b) $x_0 = (10, 10)$, weights $= (3, 5, 25, 5 \times 10^3)$.

then declines as the tumor volume decreases, and finally goes to 0 when the dose limit is reached; in Fig. 5b, the weights were tuned for a less steep response, thus conserving radiation dose and safeguarding the healthy tissue from significant toxicity.

So far, apart from the inaccuracy inherent to the first-order discretization, the internal model used by the controller has been a perfect replica of that of the system. However, in any practical scenario, the real system will differ significantly from the controller's expectations. In an effort to replicate these inaccuracies, the system model was altered in two distinct ways, without altering the controller. First, the cancer tissue's radiosensitivity parameter α_c was made to vary with time, decreasing logarithmically from an initial value of 5×10^{-2} Gy^{-1} to 5×10^{-3} Gy^{-1}; β_c changed accordingly, to maintain the tissue's characteristic α/β ratio. This scenario was simulated in the "continuous treatment" modality, and the results are presented in Fig. 6a. The controller successfully adapted to the unforeseen behavior by rapidly decreasing the dose rate at the beginning, when the tissue's sensitivity is at its highest, and increasing it slowly toward the end in an effort to compensate for the increased radiation resistance. As a second example, the cancer's proliferation rate a_c was increased by a factor of 3 compared to the original model, from 6.25×10^{-4} hour^{-1} to 1.88×10^{-3} hour^{-1}; this simulation was conducted in the pulsed regime, and is shown in Fig. 6b. Compared to a similar situation in Fig. 2a, the controller is forced to deliver a greater dose due to the cancer's faster growth, but still achieves a tumor volume

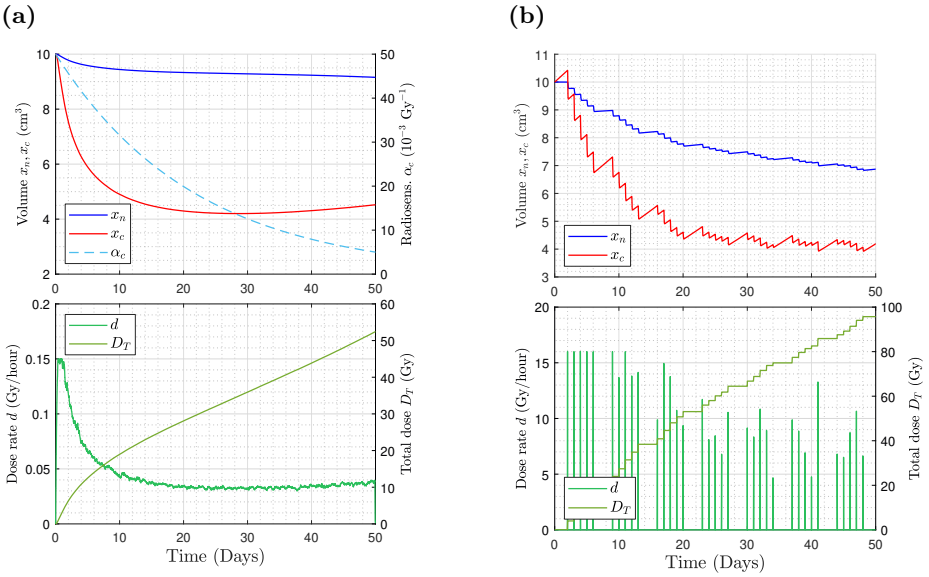

Fig. 6: Simulation of the closed-loop system with imperfect system model. (a) $x_0 = (10, 10)$, weights $= (3, 5, 25, 5 \times 10^3)$. (b) $x_0 = (10, 10)$, weights $= (1, 5, 0.5, 0)$.

steady-state starting at ~ 30 days; the greater loss of healthy cells is unavoidable in this case, not only due to the increased radiation, but also because of the cancer's more aggressive competition.

4 Conclusion

A nonlinear predictive control solution was developed for optimal cancer control in radiotherapy. By predicting the evolution of cancer and healthy tissue, the controller can compute the optimal dose that will produce the desired biological effect, while adjusting for disturbances and measurement uncertainty. To this end, a dynamical model of tumor growth, based on a first principles cell competition framework, was utilized and expanded to account for the biological effects of radiation, both immediate and delayed. Simulation results show that, with proper tuning, the controller's performance is comparable to the baseline treatment modality, even with substantial measurement uncertainty. The controller can be tuned to meet the requirements of different clinical scenarios, where the "optimal" solution will necessarily change from patient to patient. Additionally, since it is based on a feedback technique, the controller constantly adjusts itself to the current state of the system, and can compensate for unexpected behavior. This last point is especially relevant for practical application: since no high-level model can be expected to fully capture the wide range of complex dynamics that govern tumor development, the onus is then placed on the controller to effectively compensate for these inevitable discrepancies.

The time-scale of the problem does present some difficulties for controller design. The treatment window spans weeks, while the controller must operate on a time-scale of hours (or minutes). Consequently, it is generally intractable to consider prediction horizons longer than a few hours. For this reason, the controller will often produce a rather aggressive response at the start of the treatment when, in the long-term, it may have been optimal to distribute the dose more evenly. Addressing this shortcoming by utilizing two controllers, one for short-term dose delivery and another for overall treatment schedule planning, may prove a fruitful avenue for further research. Ultimately, however, control performance is limited by the accuracy of tissue measurements: highly-sensitive sensors and fast electronics for state-of-the-art imaging techniques are critical for accurately assessing the system's state, and ensuring optimal dose administration [2,14].

Meanwhile, the cancer growth model can be expanded to account for higher-order radiation effects, as well as different radiation properties. Both cell populations can also be split further into multiple variables corresponding to differentiated cell types [1]. Furthermore, the delay formulation introduced in this work is limited in practice to only a few hours, due to its complexity; future work on realizing a computationally feasible delay model on the scale of days or weeks would provide yet another degree of freedom in modelling cancer treatment dynamics.

Finally, it is yet unclear how these developments in modelling will lend themselves to automatic control strategies, or indeed the place that these controllers may occupy in actual clinical practice. Nevertheless, this work has shown the potential of applying optimal and predictive techniques to radiotherapy. Even utilizing high-level models based on simple assumptions, these tools may provide useful information to the medical professional, improve outcomes for patients, and ultimately aid in providing more effective, humane treatment procedures for one of the world's leading causes of death.

Acknowledgments. This work was financially supported by the Fundação para a Ciência e a Tecnologia (FCT) through the research grants numbers UIDB/00066/2020, UIDB/50009/2020, PTDC/EEI-AUT/1732/2020 and UID/FIS/00068/2020 (CEFITEC). JCGA further acknowledges FCT through the Ph.D. Studentship 2022.13724.BD.

Disclosure of Interests. The authors have no competing interests to declare that are relevant to the content of this article.

References

1. Radiation Biology: A Handbook for Teachers and Students. No. 42 in Training Course Series, INTERNATIONAL ATOMIC ENERGY AGENCY, Vienna (2010)
2. Albuquerque, E., Bexiga, V., Bugalho, R., Carriço, B., Ferreira, C.S., Ferreira, M., Godinho, J., Gonçalves, F., Leong, C., Lousã, P., Machado, P., Moura, R., Neves, P., Ortigão, C., Piedade, F., Pinheiro, J.F., Rego, J., Rivetti, A., Rodrigues, P., Silva, J.C., Silva, M.M., Teixeira, I.C., Teixeira, J.P., Trindade, A., Varela,

J.: Experimental characterization of the 192 channel Clear-PEM frontend ASIC coupled to a multi-pixel APD readout of LYSO:Ce crystals. Nuclear Instruments and Methods in Physics Research Section A: Accelerators, Spectrometers, Detectors and Associated Equipment **598**(3) (Jan 2009). https://doi.org/10.1016/j.nima.2008.10.005

3. Alimirzaei, I., Malek, A.: Optimal Control of Anti-Angiogenesis and Radiation Treatments for Cancerous Tumor: Hybrid Indirect Solver. Journal of Mathematics **2023** (Sep 2023). https://doi.org/10.1155/2023/5554420
4. Belostotski, G., Freedman, H.I.: A CONTROL THEORY MODEL FOR CANCER TREATMENT BY RADIOTHERAPY. International Journal of Pure and Applied Mathematics **25**(4) (2005)
5. Bertolet, A., Chamseddine, I., Paganetti, H., Schuemann, J.: The complexity of DNA damage by radiation follows a Gamma distribution: Insights from the Microdosimetric Gamma Model. Frontiers in Oncology **13** (Jun 2023). https://doi.org/10.3389/fonc.2023.1196502
6. Borrelli, F., Bemporad, A., Morari, M.: Predictive Control for Linear and Hybrid Systems. Cambridge University Press, first edn. (2017)
7. Camacho, A., Díaz-Ocampo, E., Jerez, S.: Optimal control for a bone metastasis with radiotherapy model using a linear objective functional. Mathematical Modelling of Natural Phenomena **17** (2022). https://doi.org/10.1051/mmnp/2022038
8. Connell, P.P., Hellman, S.: Advances in Radiotherapy and Implications for the Next Century: A Historical Perspective. Cancer Research **69**(2) (Jan 2009). https://doi.org/10.1158/0008-5472.CAN-07-6871
9. Freedman, H.I., Belostotski, G.: Perturbed models for cancer treatment by radiotherapy. Differential Equations and Dynamical Systems **17**(1-2) (Apr 2009). https://doi.org/10.1007/s12591-009-0009-7
10. Jiao, Y., Cao, F., Liu, H.: Radiation-induced Cell Death and Its Mechanisms. Health Physics **123**(5) (Nov 2022). https://doi.org/10.1097/HP.0000000000001601
11. Krishnan, J., Rao, S., Hegde, S., Shetty, J.: Evaluation of healthy tissue dose at different regions between volumetric-modulated arc therapy and intensity-modulated radiation therapy plans in the treatment of various cancers. Journal of Medical Physics **44**(3) (2019). https://doi.org/10.4103/jmp.JMP_122_18
12. Lotka, A.J.: The growth of mixed populations: Two species competing for a common food supply. Journal of the Washington Academy of Sciences **22**(16/17) (1932)
13. McMahon, S.J.: The linear quadratic model: Usage, interpretation and challenges. Physics in Medicine & Biology **64**(1) (Dec 2018). https://doi.org/10.1088/1361-6560/aaf26a
14. Pereira, G.C., Traughber, M., Muzic, R.F.: The Role of Imaging in Radiation Therapy Planning: Past, Present, and Future. BioMed Research International **2014** (Apr 2014). https://doi.org/10.1155/2014/231090
15. Smith, H.: An Introduction to Delay Differential Equations with Applications to the Life Sciences, Texts in Applied Mathematics, vol. 57. Springer New York, New York, NY (2011). https://doi.org/10.1007/978-1-4419-7646-8
16. Wilson, N., Drapaca, C.S., Enderling, H., Caudell, J.J., Wilkie, K.P.: Modelling Radiation Cancer Treatment with a Death-Rate Term in Ordinary and Fractional Differential Equations. Bulletin of Mathematical Biology **85**(6) (Jun 2023). https://doi.org/10.1007/s11538-023-01139-2